International Journal of Mathematical Archive-5(4), 2014, 127-136
Available online through www.ijma.info ISSN 2229 – 5046

EFFECT OF QUADRATIC DENSITY TEMPERATURE VARIATION ON UNSTEADY CONVECTIVE HEAT AND MASS TRANSFER FLOW IN VERTICAL CHANNEL

P. Raja kumari*[1] and A. Leela Ratnam[2]

[1]Research Scholar, Dept. of. Applied Mathematics, SPMVV, Tirupati. India.
[2]Professor, Dept. of. Applied Mathematics, SPMVV, Tirupati. India.

(Received on: 20-03-14; Revised & Accepted on: 04-04-14)

ABSTRACT

In this paper we investigate the unsteady convective heat and mass transfer flow of a viscous fluid through a porous medium in a vertical channel on whose walls a travelling thermal wave is imposed with quadratic temperature variation. The governing equations are solved by using Regular perturbation scheme. The velocity, temperature, stress and rate of heat transfer on the boundaries are evaluated numerically for different variations of governing parameters. The graphs are drawn for different variations and the results are discussed in detail.

Key words: *Quadratic temperature variation, Heat and Mass transfer, Porous medium, Traveling thermal wave.*

1. INTRODUCTION

The effects of radiation on MHD flow and heat transfer problem have become more important industrially. Many processes in engineering areas occur at high temperature, and knowledge of radiation heat transfer becomes very important for the design of the pertinent equipment. Nuclear power plants, Gas turbines and various propulsion devices, for aircraft, missiles, satellites and space vehicles are examples of such engineering areas.

Radiative flow plays a vital role in many industrial and environmental process e.g. heating and cooling chambers, fossil fuel combustion energy process, evaporation form larger open water reservoirs, ,astrophysical flows, solar power technology and space vehicle re-entry

Sastri and Vajravelu [1] have solved the problem of free convection between vertical walls by taking the non-linear density temperature variation. Bhargawa and Agarwal [2] have investigated the fully developed laminar free convection flow in the presence of constant heat sources in a circular pipe taking the same density temperature relationship. Following a quadratic density temperature variation Gupta, Dubey and Sharma [3] have discussed the laminar free convection flow through coaxial circular cylinders with and without heat sources.

Nagaraja [4] has investigated the combined heat and mass transfer effects on the flow of a viscous fluid through a porous medium in a vertical channel, with the travelling thermal waves imposed on the boundaries while the concentration is maintained uniform on the boundaries.

Purushothama Reddy [5] has analyzed the unsteady mixed convection effects on the flow of incompressible viscous fluid in vertical wavy channel. The Thermal buoyancy in the flow field is created by a traveling thermal wave imposed on the boundaries. Taking non-linear density temperature variation Sarojamma [6] has analysed the hydromagnetic free convection flow in a cylindrical geometry. Sivanjaneya Prasad [7] has analysed the combined heat and mass transfer effects on the flow of an incompressible electrically conducting viscous fluid through a porous medium in a vertical channel.

Sreenivasa Reddy [8] has analyzed the Soret effect on unsteady convective heat and mass transfer through a porous medium in a vertical channel. Ravindrananth [9] has discussed the dissipative effect on MHD free convective flow through a porous medium in a vertical channel. The unsteadiness in the flow is due to the traveling thermal wave imposed on the wall y = L under a uniform magnetic field. The coupled equations governing the flow and heat transfer have been solved by using a perturbation technique with the aspect ratio as perturbation parameter.

Corresponding author: P. Raja kumari[1]*
[1]Research Scholar, Dept. of. Applied Mathematics, SPMVV, Tirupati. India.
E-mail: rajakumari258@gmail.com

Bharathi [10] has discussed the combined influence of dissipation and Soret effects on convective heat and mass transfer of a viscous incompressible fluid through a porous medium in a vertical channel bounded flat walls. The thermal buoyancy in the flow field is created by a travelling thermal wave imposed on the boundary wall at y = L while the boundary at y = -L is imposed at constant temperature T_1. Recently Aliveni [11] has studied convective heat and mass transfer flow of a viscous electrically conducting fluid in a vertical channel with quadratic temperature variation in the presence of heat sources.

2. FORMULATION OF THE PROBLEM

We consider the motion of viscous fluid in a vertical channel bounded by flat walls. The thermal buoyancy in the flow field is created by a traveling thermal wave imposed on the boundary wall at y=L while the boundary at y = -L is maintained at constant temperature T_1. The walls are maintained at constant concentrations. The Boussinesq approximation is used so that the density variation will be considered only in the buoyancy force. A uniform magnetic field of strength Ho is applied normal to the walls. Assuming the magnetic Reynolds number to be small we neglect the induced magnetic field in comparision with the applied fied. Also the kinematic viscosity ν, the thermal conducting k are treated as constants. We choose a rectangular Cartesian system 0 (x, y) with x-axis in the vertical direction and y-axis normal to the walls. The walls of the channel are at y = ± L.A uniform magnetic field of strength Ho is applied normal to the wall.

The equations governing the unsteady flow, heat and mass transfer are

Equation of linear momentum

$$\rho_e\left(\frac{\partial u}{\partial t}+u\frac{\partial u}{\partial x}+v\frac{\partial u}{\partial y}\right)=-\frac{\partial p}{\partial x}+\mu\left(\frac{\partial^2 u}{\partial x^2}+\frac{\partial^2 u}{\partial y^2}\right)-\rho g-\left(\frac{\sigma\mu_e^2 H_o^2}{\rho}\right)u \tag{2.1}$$

$$\rho_e\left(\frac{\partial v}{\partial t}+u\frac{\partial v}{\partial x}+v\frac{\partial v}{\partial y}\right)=-\frac{\partial p}{\partial y}+\mu\left(\frac{\partial^2 v}{\partial x^2}+\frac{\partial^2 v}{\partial y^2}\right) \tag{2.2}$$

Equation of continuity

$$\frac{\partial u}{\partial x}+\frac{\partial v}{\partial y}=0 \tag{2.3}$$

Equation of energy

$$\rho_e C_p\left(\frac{\partial T}{\partial t}+u\frac{\partial T}{\partial x}+v\frac{\partial T}{\partial y}\right)=\lambda\left(\frac{\partial^2 T}{\partial x^2}+\frac{\partial^2 T}{\partial y^2}\right)+Q-\frac{\partial q_r}{\partial y} \tag{2.4}$$

Equation of diffusion

$$\left(\frac{\partial C}{\partial t}+u\frac{\partial C}{\partial x}+v\frac{\partial C}{\partial y}\right)=D\left(\frac{\partial^2 C}{\partial x^2}+\frac{\partial^2 C}{\partial y^2}\right)+k_{11}\left(\frac{\partial^2 T}{\partial x^2}+\frac{\partial^2 T}{\partial y^2}\right) \tag{2.5}$$

Equation of state

$$\rho=\rho_e(1-\beta(T-T_o)^2-\beta^{\bullet}(C-C_o))$$

By using Rosseland approximation (3a) the radiative heat flux is given by

$$q_r=-\frac{4\sigma^{\bullet}}{3\beta_R}\frac{\partial T'^4}{\partial y} \tag{2.5a}$$

and by Taylor's expansion we get

$T'^4 \cong 4T_e^3 T-3T_e^4$ after neglecting higher order terms. (2.5b)

$\sigma^{\bullet}$ is the Stefan-Boltzmann constant and β_R is the mean absorption coefficient.

In the equilibrium state

$$0=-\frac{\partial p_e}{\partial x}-\rho_e g \tag{2.6}$$

© 2014, IJMA. All Rights Reserved

where $p = p_e + p_D$, p_D being the hydrodynamic pressure.

The flow is maintained by a constant volume flux for which a characteristic velocity is defined as

$$Q = \frac{1}{2L}\int_{-L}^{L} u \, d\,y. \tag{2.7}$$

The boundary conditions for the velocity and temperature fields are

u = 0, v = 0, $T=T_1$, $C=C_1$ on y = -L

$$u = 0,\ v = 0, T = T_2 + (T_1 - T_2)\,Sin(mx + nt),\ C=C_2 \text{ on } y = +L \tag{2.8}$$

where $Sin(mx + nt)$ is the imposed traveling thermal wave

In view of the continuity equation we define the stream function ψ as

$$u = -\psi_y,\ v = \psi_x \tag{2.9}$$

Eliminating pressure p from equations (2.1) & (2.2) and using the equations (2.4) and (2.5) governing the flow in terms of ψ are

$$[(\nabla^2\psi)_t + \psi_x(\nabla^2\psi)_y - \psi_y(\nabla^2\psi)_x] = \nu\nabla^4\psi - 2\beta\, g(T - T_0)(T - T_0)_y - \beta^{\bullet}(C - C_o) - \left(\frac{\sigma\mu_e^2 H_o^2}{\rho}\right)\frac{\partial^2\psi}{\partial y^2} \tag{2.10}$$

$$\rho_e C_p\left(\frac{\partial T}{\partial t} + \frac{\partial\psi}{\partial y}\frac{\partial T}{\partial x} - \frac{\partial\psi}{\partial x}\frac{\partial T}{\partial y}\right) = \lambda\nabla^2 T + Q + \frac{16\sigma^{\bullet}T_e^3}{3\beta_R}\frac{\partial^2 T}{\partial y^2} \tag{2.11}$$

$$\left(\frac{\partial C}{\partial t} + \frac{\partial\psi}{\partial y}\frac{\partial C}{\partial x} - \frac{\partial\psi}{\partial x}\frac{\partial C}{\partial y}\right) = D\nabla^2 C + K_{11}\nabla^2 T \tag{2.12}$$

Introducing the non-dimensional variables in (2 .10)-(2.12) as

$$x' = mx,\ y' = y/L, t' = t\nu m^2, \Psi' = \Psi/\nu, \theta = \frac{T - T_2}{(T_1 - T_2)}, C' = \frac{C - C_2}{(C_1 - C_2)} \tag{2.13}$$

The governing equations in the non-dimensional form (after dropping the dashes) are

$$\delta R\left(\delta(\nabla_1^2\psi)_t + \frac{\partial(\psi, \nabla_1^2\psi)}{\partial(x, y)}\right) = \nabla_1^4\psi - \frac{2G}{R}(\theta\,\theta_y) - M^2\frac{\partial^2\psi}{\partial y^2} \tag{2.14}$$

$$\delta P_1\left(\delta\frac{\partial\theta}{\partial t} + R\left(\frac{\partial\psi}{\partial y}\frac{\partial\theta}{\partial x} - \frac{\partial\psi}{\partial x}\frac{\partial\theta}{\partial y}\right)\right) = \nabla_1^2\theta + \alpha_1 \tag{2.15}$$

$$\delta Sc\left(\delta\frac{\partial C}{\partial t} + R\left(\frac{\partial\psi}{\partial y}\frac{\partial C}{\partial x} - \frac{\partial\psi}{\partial x}\frac{\partial C}{\partial y}\right)\right) = \nabla_1^2 C + \frac{Sc\,S_0}{N_1}\theta_{yy} \tag{2.16}$$

where

$R = \frac{UL}{\nu}$ (Reynolds number) $\quad So = \frac{k_{11}\beta^{\bullet}}{\nu\beta}$ (Soret parameter)

$G = \frac{\beta g\Delta T_e L^3}{\nu^2}$ (Grashof number) $\quad N_1 = \frac{3\beta_R\lambda}{4\sigma^{\bullet}T_e^3}$ (Radiation parameter)

$P = \frac{\mu c_p}{k_1}$ (Prandtl number), $\quad P_1 = \frac{3N_1 P}{3N_1 + 4} \quad \alpha_1 = \frac{3N_1\alpha}{3N_1 + 4}$

$\delta = m\,L$ (Aspect ratio) $\quad \nabla_1^2 = \delta^2\frac{\partial^2}{\partial x^2} + \frac{\partial^2}{\partial y^2}$

© 2014, IJMA. All Rights Reserved

$\gamma = \dfrac{n}{\nu m^2}$ (Non-dimensional thermal wave velocity)

$Sc = \dfrac{\nu}{D}$ (Schimdt Number) $u = \dfrac{-\partial\psi}{\partial y}, v = \dfrac{\partial\psi}{\partial x}$

The corresponding boundary conditions are

$$\psi(+1) - \psi(-1) = -1$$

$$\frac{\partial\psi}{\partial x} = 0, \quad \frac{\partial\psi}{\partial y} = 0 \ at\ y = \pm 1 \tag{2.15}$$

$\theta(x, y) = 1,\ C(x, y) = 1$ on y = -1

$\theta(x, y) = Sin(x + \gamma t) \quad C(x, y) = 0$ on y = 1

$$\frac{\partial\theta}{\partial y} = 0 \ \ at \ \ y = 0 \tag{2.16}$$

The value of ψ on the boundary assumes the constant volumetric flow in consistent with the hypothesis (2.7) .Also the wall temperature varies in the axial direction in accordance with the prescribed arbitrary function t .

3. ANALYSIS OF THE FLOW

The main aim of the analysis is to discuss the perturbations created over a combined free and forced convection flow due to traveling thermal wave imposed on the boundaries. The perturbation analysis is carried out by assuming that the aspect ratio δ to be small.

We adopt the perturbation scheme and write

$$\psi(x, y, t) = \psi_0(x, y.t) + \delta\psi_1(x, y, t) + \delta^2\psi_2(x, y, t) + ...$$
$$\theta(x, y, t) = \theta_0(x, y, t) + \delta\,\theta_1(x, y, t) + \delta^2\,\theta_2(x, y, t) + ...$$
$$C(x, y, t) = C_0(x, y, t) + \delta\,C_1(x, y, t) + \delta^2\,C_2(x, y, t) + ... \tag{3.1}$$

On substituting (3.1) in (2.14) - (2.16) and separating the like powers of δ the equations and respective conditions to the zeroth order are

$$\psi_{0,\,yyyyy} - M_1^2\psi_{0,\,yy} = G(2\theta_o\,\theta_{o,y} + N\,C_{oy})/R \tag{3.2}$$

$$\theta_{o,yy} = -\alpha_1 \tag{3.3}$$

$$C_{o,yy} = -\frac{Sc\,So}{N}\theta_{o,yy} \tag{3.4}$$

with

$\psi_0(+1)-\Psi(-1) = -$,

$\psi_{0,y} = 0,\ \psi_{0,x} = 0$ on y = ±1 (3.5)

$$\theta_o = 1, C_o = 1 \ \ on \quad y = -1$$

$$\theta_o = Sin(x + \gamma t) \quad Co = 0 \quad on\ y = 1 \tag{3.6}$$

and to the first order are

$$\psi_{1,\,yyyyy} - M_1^2\psi_{1,\,yy} = G(2(\theta_o\theta_{1,yy} + \theta_1\,\theta_{o,y}) + \theta_{1,y} + NC_{1.y})/R + (\psi_{0,\,y}\,\psi_{0,\,xyy} - \psi_{0,\,x}\,\psi_{0,yyy}) \tag{3.7}$$

$$\theta_{1,yy} = RP_1(\psi_{0,x}\theta_{o,y} - \psi_{0,y}\theta_{ox}) \tag{3.8}$$

$$C_{1,yy} = -\frac{ScSo}{N}\ \theta_{1,yy} \tag{3.9}$$

with

$\psi_{1(+1)} - \psi_{1(-1)} = 0$

$\psi_{1,y=}0,\ \psi_{1,x} = 0$ on $y = \pm 1$ (3.10)

$\theta_1(\pm 1) = 0,\ C_1(\pm 1) = 0$ on $y = \pm 11$ (3.11)

4. SOLUTION OF THE PROBLEM

Solving the equations (3.2) - (3.9) subject to the relevant boundary conditions we obtain

$$\theta_o(y,t) = -\left(\frac{\alpha_1}{2}\right)(1-y^2) + \left(\frac{Sin(D_1)}{2}\right)(1-y) + 0.5\,(y+1)$$

$$C_o(y,t) = 0.5a_3(y^2-1) + 0.5(y+1)$$

$$\theta_1(y) = a_7y^4 + a_8y^3 + a_9y^2$$

$$\psi_o(y,t) = a_{13} + a_{12}y + a_{10}Ch(M_1y) + a_{11}Sh(M_1y) + \varphi(y)$$

$$C_1(y,t) = 0.5a_{31}(y^2-1) + a_{30}(y^3-y)/6 + a_{29}(y^4-1)/12 + a_{28}(y^5-y)/20 + a_{27}(y^6-1)/30$$
$$+a_{26}(y^7-y)/42 + a_{25}(Ch(M_1y) - Ch(M_1)/M_1^2 + a_{24}(Sh(M_1y) - ySh(M_1))$$

$$\psi_1 = B_1 + B_2y + B_3Ch(M_1y) + B_4Sh(M_1y) + \varphi_1(y)$$

$$\varphi_1(y) = a_{76}y + a_{75}y^2 + a_{74}y^3 + a_{73}y^4 + a_{72}y^5 + a_{71}y^6 + a_{70}y^7 + a_{69}y^8$$
$$+a_{68}y^9 + a_{67}y^{10} + (a_{65} + ya_{63} + y^2a_{61} + y^3a_{53} + y^4a_{57})Ch(M_1y)$$
$$+(a_{66} + ya_{64} + y^2a_{62} + y^3a_{60} + y^4a_{58})Sh(M_1y)$$

where $a_1, a_2, \ldots\ldots\ldots\ldots a_{74}, B_1, B_2, \ldots\ldots\ldots\ldots B_4$ are constants given in the appendix

5. SHEAR STRESS, NUSSELT NUMBER AND SHERWOOD NUMBER

The shear stress on the channel walls is given by

$$\tau = \mu\left(\frac{\partial u}{\partial y} + \frac{\partial v}{\partial x}\right)_{y=\pm L}$$

The local rate of heat transfer coefficient (Nusselt number Nu) on the walls has been calculated using the formula

$$Nu = \frac{1}{\theta_m - \theta_w}\left(\frac{\partial \theta}{\partial y}\right)_{y=\pm 1}$$

The local rate of mass transfer coefficient (Sherwood number Sh) on the walls has been calculated using the formula

$$Sh = \frac{1}{C_m - C_w}\left(\frac{\partial C}{\partial y}\right)_{y=\pm 1}$$

© 2014, IJMA. All Rights Reserved

6. DISCUSSION OF THE NUMERICAL RESULTS

In this analysis we discuss the effect of radiation on unsteady convective heat and mass transfer flow of a viscous fluid through a porous medium in a vertical channel. The unsteadiness in the flow is due to a traveling thermal wave imposed on the walls. Analysis has been carried out with P = 0.71.The velocity distribution is shown in figures 1-9 in different variations of G, R, D^{-1}, Sc, α, N_1 and $x+\gamma t$.

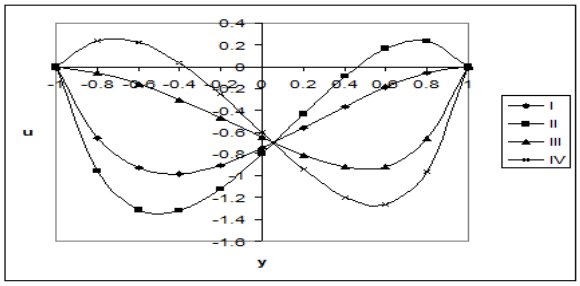

Fig. - 1: Variation of u with G

	I	II	III	IV
G	10^3	$3x10^3$	-10^3	$-3x10^3$

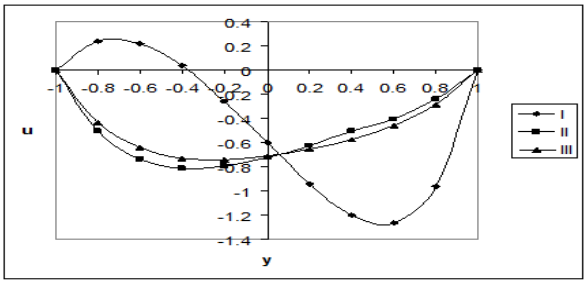

Fig. - 2: Variation of u with R

	I	II	III
R	35	70	140

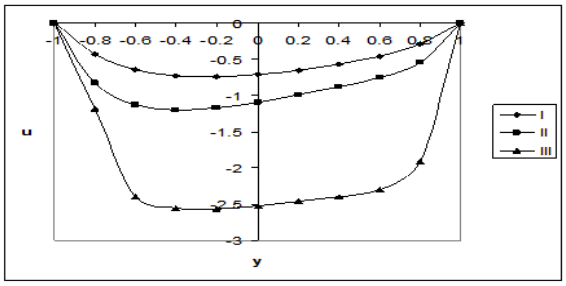

Fig. - 3: Variation of u with D^{-1}

	I	II	III
D^{-1}	100	200	300

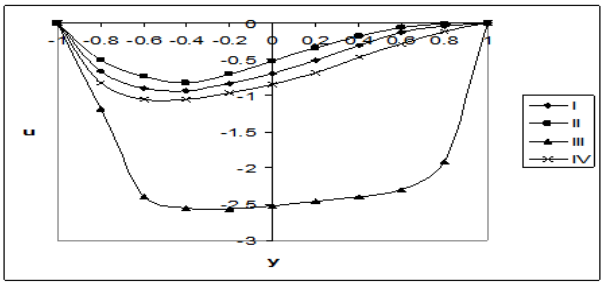

Fig. - 4: Variation of u with Sc

	I	II	III	IV
Sc	0.24	0.6	1.3	2.01

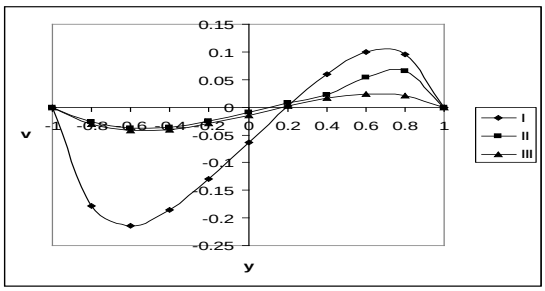

Fig. - 5: Variation of v with R

	I	II	III
R	35	70	140

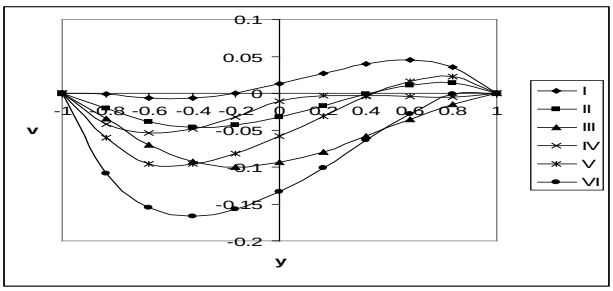

Fig. - 6: Variation of v with α

	I	II	III	IV	V	VI
α	2	4	6	-2	-4	-6

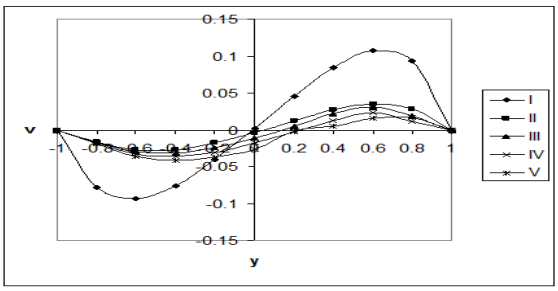

Fig. - 7: Variation of v with N_1

	I	II	III	IV	V
N_1	1.50	2.50	5.00	10.00	100.00

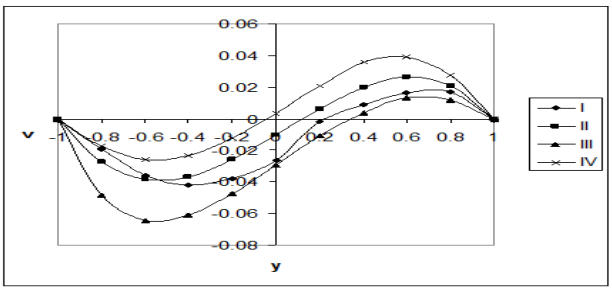

Fig. - 8: Variation of v with $x+\gamma t$

	I	II	III	IV
$x+\gamma t$	$\pi/4$	$\pi/2$	π	2π

© 2014, IJMA. All Rights Reserved

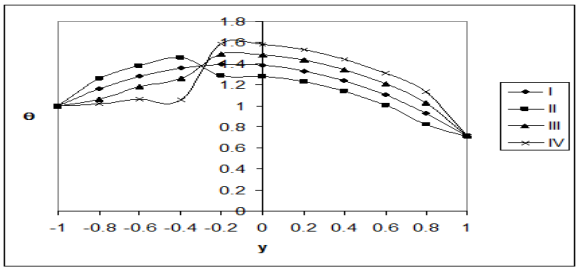

Fig. - 9: Variation of θ with G

	I	II	III	IV
G	10^3	$3x10^3$	-10^3	$-3x10^3$

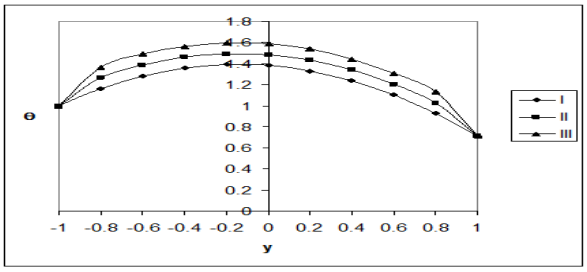

Fig. - 10: Variation of θ with R

	I	II	III
R	35	70	140

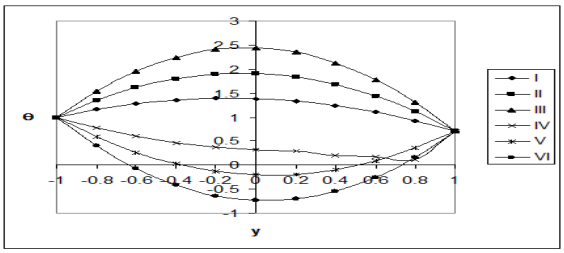

Fig. - 11: Variation of θ with α

	I	II	III	IV	V	VI
α	2	4	6	-2	-4	-6

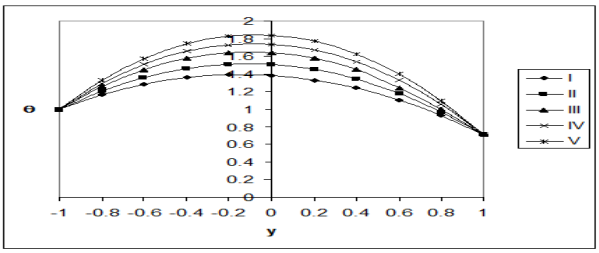

Fig. - 12: Variation of θ with N_1

	I	II	III	IV	V
N_1	1.50	2.50	5.00	10.00	100.00

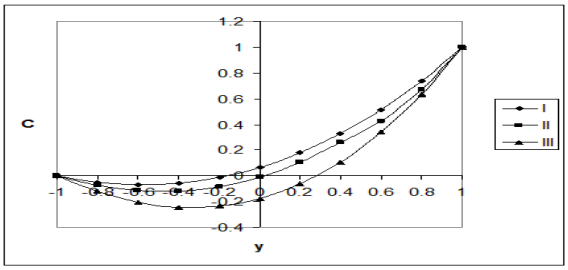

Fig. - 13: Variation of C with R

	I	II	III
R	35	70	140.

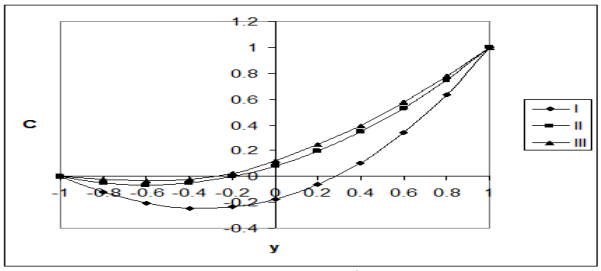

Fig. - 14: Variation of C with D^{-1}

	I	II	III
D^{-1}	100	200	300

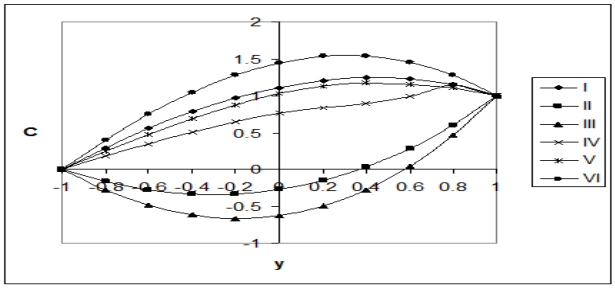

Fig. - 15: Variation of C with α

	I	II	III	IV	V	VI
α	2	4	6	-2	-4	-6

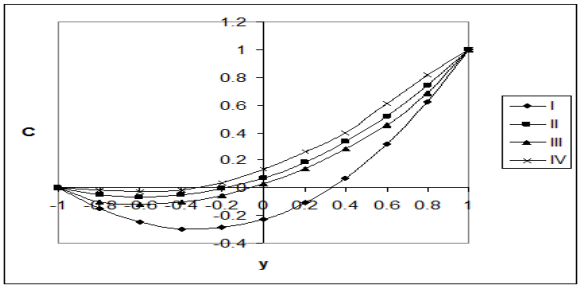

Fig. - 16: Variation of C with x+γt

	I	II	III	IV
x+γt	π/4	π/2	π	2π

Fig. 1 represents variation of u with Grashof number G. It is found that for G > 0, u exhibits a reversal flow in a narrow region adjacent to y = 1 and for G < 0 it occurs in the region $-0.8 \le y \le -0.4$ also the magnitude of u enhances in the flow region. An increase in the Reynolds number $R \le 70$ enhances |u| and depreciates with higher $R \ge 140$. The reversal flow which appears in the left half for R = 35 and disappears for higher values of R (fig. 2). Fig. 3 represents the variation of u with Darcy parameter $D^{-1.}$ It is found that lesser the permeability of the porous medium larger |u| in the flow region with maximum attained at y = -0.4. The variation of u with Schmidt number Sc shows that lesser the molecular diffusivity smaller |u| and for further lowering of the molecular diffusivity larger |u| in the region and for still lowering of the molecular diffusivity smaller |u| in the flow region (fig. 4).

An increase in Reynolds number R enhances |v| in the left half and reduces in the right half (fig.11). An increase in the heat source parameter α enhances |v| in the entire flow region (fig. 15). The variation of v with the radiation parameter N_1 exhibits a different nature on v. An increase in $N_1 \le 2.5$ reduces |v| in the entire flow region and for higher $N_1 \ge 5$, |v| enhances in the right half (fig. 17). An increase in the phase $x+\gamma t \le \pi/2$, |v| reduces in the left half and enhances in the right half, while for higher $x+\gamma t \ge \pi$, |v| enhances in the right half and reduces in the left half (fig. 18). Fig. 19 represents the variation of θ with Grashof number G. It is found that the actual temperature reduces with increase in $G > 0$ except in the region $-0.8 \le y \le -0.4$ where it enhances. For an increase in $G < 0$ we notice an enhancement in θ except in the region $-0.8 \le y \le -0.4$ where it depreciates. An increase in $R \le 70$ reduces θ in the right half and enhances in the left half and for higher $R \ge 140$ it enhances in the left half and reduces in the right half (fig. 20). The variation of θ with heat source parameter α is shown in fig. 23. It is found that an increase in the strength of the heat source enhances the actual temperature in the flow field and in the case of heat sink the actual temperature depreciates with $|\alpha|$. The influence of the radiative heat transfer on θ is shown in fig. 25. It is found that higher the radiative heat flux larger the actual temperature. An increase in the Reynolds number R depreciates the actual concentration in the entire flow region (fig. 28). The variation of C with D^{-1} shows that higher the Lorentz force larger the actual concentration and for further higher Lorentz force larger the actual concentration in the right half and smaller the concentration in the left half (fig.29). The influence of heat source on C is shown in Fig. 32. An increase in $\alpha > 0$ reduces the actual concentration while it enhances with increase in $|\alpha|$. An increase in the phase $x+\gamma t \le \pi/2$ of the traveling thermal wave enhances the actual concentration and reduces with higher $x+\gamma t = \pi$ and again enhances with the still higher value $x+\gamma t = 2\pi$ (fig. 35).

Table - 1
Variation of Shear stress τ at y = +1

G	I	II	III	IV	V
10^3	-32.16890	-25.18176	-21.67874	-26.2492	-76.1200
$3x10^3$	-46.13057	-32.16260	-25.16916	-115.2492	-157.0856
-10^3	-4.24556	-11.22009	-14.69790	-46.53078	-86.9642
$-3x10^3$	9.71611	-14.23926	-21.20749	110.39930	414.39910
R	35	70	140	35	35
D^{-1}	100	100	100	2X100	3X100

Table - 2
Variation of Shear stress τ at y = -1

G	I	II	III	IV	V
10^3	4.42335	3.36718	2.85843	4.31838	4.49496
$3x10^3$	6.57854	4.44496	3.39737	5.81359	6.70595
-10^3	0.16361	1.23731	1.79349	1.34468	2.08187
$-3x10^3$	-1.94094	2.18522	3.26750	-0.13380	0.88008
R	35	70	140	35	35
D^{-1}	100	100	100	2X100	3X100

It is found that the stress enhances with increase in |G| at $y = \pm 1$. An increase in the Reynold's number R reduces $|\tau|$ in the heating case and enhances in the cooling case at both the walls. The variation of τ with Darcy parameter D^{-1} shows that higher the Lorentz smaller $|\tau|$ at y= -1 while it enhances at y = +1 (tables 1 & 2)

Table - 3
Variation of Shear stress τ at y = +1

G	I	II	III	IV	V	VI	VII
10^3	-26.30618	-35.24633	-39.36189	-42.61579	-5.16561	18.02613	-23.99666
$3x10^3$	-34.39380	-49.44659	-54.50267	-58.86267	-2.24702	17.60119	-29.10448
-10^3	-4.13097	-6.84581	-9.08030	-10.12201	-11.00279	18.87601	-13.78102
$-3x10^3$	-2.04335	-4.1256	6.06049	6.12488	-13.92138	19.30095	-9.67319
N_1	1.50	2.50	5.00	10.00	1.50	1.50	1.50
$x+\gamma t$	$\pi/4$	$\pi/4$	$\pi/4$	$\pi/4$	$\pi/2$	π	2π

© 2014, IJMA. All Rights Reserved

Table - 4
Variation of Shear stress τ at y = -1

G	I	II	III	IV	V	VI	VII
10^3	3.84065	4.61761	4.83718	4.98804	5.17578	2.75379	3.32258
$3x10^3$	5.43639	6.99255	7.46703	7.79870	8.09599	3.27885	4.37591
-10^3	0.19979	-0.29713	-0.40876	-0.63050	-0.01952	1.77098	1.27684
$-3x10^3$	-0.84531	-1.2452	-3.02485	-3.43839	-3.49461	1.31322	0.28444
N_1	1.50	2.50	5.00	10.00	1.50	1.50	1.50
$x+\gamma t$	$\pi/4$	$\pi/4$	$\pi/4$	$\pi/4$	$\pi/2$	π	2π

Also an increase in radiation parameter N_1 results in an enhancement at y = ±1. The variation of τ with phase $x+\gamma t$ shows that at y = -1, $|\tau|$ depreciates with $x+\gamma t \leq \pi/2$ and enhances with higher $x+\gamma t \geq \pi$ for G > 0 and for G < 0 it enhances with $x+\gamma t \leq \pi$ and reduces with $x+\gamma t \geq 2\pi$. At y= +1 an increase in $x+\gamma t \leq \pi/2$ enhances $|\tau|$, depreciates with $x+\gamma t = \pi$ and again at $x+\gamma t = 2\pi$, $|\tau|$ enhances with G > 0 and depreciates with G < 0 (tables 3 & 4).

Table - 5
Variation of Nusselt number (Nu) at y = +1

G	I	II	III	IV	V	VI
10^3	1.95829	1.95745	1.95274	1.95413	1.96187	1.96488
$3x10^3$	1.93053	1.92883	1.91927	1.92211	1.93774	1.94373
-10^3	2.01369	2.01451	2.01906	2.01773	2.01014	2.00712
$-3x10^3$	2.04133	2.04296	2.05191	2.04929	2.03427	2.02823
Sc	0.24	0.60	1.30	2.01	1.30	1.30
S_0	0.50	0.50	1.00	0.50	-0.50	-1.00

Table - 6
Variation of Nusselt number (Nu) at y = -1

G	I	II	III	IV	V	VI
10^3	-2.18472	-2.18426	-2.18170	-2.18246	-2.18668	-2.18831
$3x10^3$	-2.19590	-2.19497	-2.18976	-2.19131	-2.19982	-2.20308
-10^3	-2.16232	-2.16277	-2.16526	-2.16453	-2.16039	-2.15874
$-3x10^3$	-2.15110	-2.15199	-2.15689	-2.15546	-2.14724	-2.14393
Sc	0.24	0.60	1.30	2.01	1.30	1.30
S_0	0.50	0.50	1.00	0.50	-0.50	-1.00

The variation of Nu with Schmidt number Sc shows that lesser the molecular diffusivity smaller |Nu| and for further lowering of the molecular diffusivity larger |Nu| at y = ±1 in the heating case while in the cooling case a reversed behavior is noticed in |Nu| at both the walls. An increase in the Soret parameter $S_0 > 0$ depreciates |Nu| at y = -1 and enhances at y = +1, while an increase in $|S_0|$ enhances |Nu| for G < 0 and reduces |Nu| for G > 0 at both the walls.

Table - 7
Variation of Sherwood number (Sh) at y = +1

G	I	II	III	IV	V	VI	VII	VIII	IX
10^3	3.66611	-1.02355	-1.14589	0.30151	3.36333	-13.93542	-0.68056	3.10695	0.62972
3x10	3.88770	-1.02256	-1.14219	0.32720	3.41483	-16.63235	-0.68125	2.81143	0.59867
-10^3	3.28726	-1.02569	-1.16189	0.25789	3.26561	-10.40996	-0.67966	3.91393	0.70118
-3x1(	3.12425	-1.02684	-1.17440	0.23954	3.21923	-9.21254	-0.67945	4.48162	0.74223
α	2	4	6	-2	-4	-6	2	2	2
N	1	1	1	1	1	1	2	-0.50	-0.80

Table - 8
Variation of Sherwood number (Sh) at y = -1

G	I	II	III	IV	V	VI	VII	VIII	IX
10^3	1.98403	0.79012	0.91768	3.26957	2.00031	1.73056	0.07852	2.07402	2.86379
$3x10^3$	1.95772	0.78937	0.91743	3.08185	1.99264	1.75738	0.07093	2.14283	2.99514
-10^3	2.04032	0.79191	0.93311	3.74685	2.01605	1.68542	0.09475	1.95473	2.64056
$-3x10^3$	2.07044	0.79297	0.94891	4.05428	2.02412	1.66692	1.10335	1.90300	2.54532
α	2	4	6	-2	-4	-6	2	2	2
N	1	1	1	1	1	1	2	-0.50	-0.80

© 2014, IJMA. All Rights Reserved

The variation of Sh with α shows that |Sh| reduces with increase in $\alpha \leq 4$ and enhances with $|\alpha| \geq 6$ where it enhances at y = +1 and reduces at y = -1 with increase in $|\alpha|$. The rate of mass transfer depreciates at y = ±1 with increase in N > 0 and for N < 0, |Sh| reduces at y = +1 and enhances at y = -1.

7. REFERENCES

1. Sastry and Vajravelu: J. Fluid Mech. v.86, pp.365-383 (1978).
2. Bhargava, R and Agarwal, R.S: Ind. J. pure and Appl. Maths 10(3), p. 357, (1979).
3. Gupta, M. Dubey, G.K. and Sarma M.S.: Ind. J. Purre and Appl. Maths, 10 (7), p.792 (1979).
4. Nagaraja,P: Heat and Mass transportation in time dependent flows through channels, Ph.D. Thesis, S.K. University, Anantapur, India, (1993).
5. Purushothama Reddy Y, Prasada Rao D.R.V.: Unsteady mixed convective flows through vertical channel with varying gap, Ph.D. thesis, S. K. University, Anantapur, A.P., India, (1995).
6. Sarojamma, G. Ph.D. Thesis, University, Anantapur, (1981).
7. Sivanjaneya Prasad, P: Effects of convective Heat and Mass transfer on unsteady hydromagnetic channel. Flows, Ph.D. Thesis, S.K. University, Anantapur, India (2001)
8. Sreenivasa Reddy,B: Thermo-Diffusion effect on convective Heat and Mass transfer through a porous medium, Ph.D. Thesis, S.K. University Anantapur, India (2006).
9. Ravindranath,P: Buoyancy induced Hydromagnetic flows through a porous medium with dissipative effects, Ph.D. Thesis submitted to S. K. University, Anantapur, India, (2006).
10. Bharathi, K.: convective Heat and Mass Transfer through a porous medium in channels/pipes with radiation and Soret effects, Ph.D. Thesis, S.K. University Anantapur, India, (2007).
11. Alivene, B: Effect of radiation on Mhd convective heat and mass transfer Flow of a viscous electrically conducting fluid in a vertical channel with heat sources, M. Phil dissertation, S.K. University, Anantapur, (2010).

Source of support: Nil, Conflict of interest: None Declared